Preparations of CaRuO3 body by plasma sintering and its thermoelectric properties

Materials Transactions, Vol. 48, No. 6 (2007) pp. 1529 to 1533

Preparations of $CaRuO_3$ Body by Plasma Sintering and Its Thermoelectric Properties

Nittaya Keawprak, Rong Tu and Takashi Goto

Institute for Materials Research, Tohoku University, Sendai 980-8577, Japan

Dense $CaRuO_3$ body was synthesized by spark plasma sintering (SPS) using $CaCO_3$ and RuO_2 powders. The second phases of CaO and RuO_2 were identified at the Ru to Ca molar ratio in the source powder ($R_{Ru/Ca}$) of 0.5 to 0.8 and at $R_{Ru/Ca} = 1.1$ to 1.4, respectively. A non-stoichiometric solid solution range of bulk $CaRuO_3$ body was first found in the $R_{Ru/Ca}$ range between 0.7 and 1.0. The density increased with increasing $R_{Ru/Ca}$ and the highest density was 97% at $R_{Ru/Ca} = 1.4$. The electrical conductivity (σ) decreased with increasing temperature, showing a metallic conduction behavior. The σ increased from 1×10^5 to 5×10^5 Sm^{-1} with increasing $R_{Ru/Ca}$ at room temperature (RT). The Seebeck coefficient (S) was around 25 to 35 μVK^{-1} from RT to 1023 K independent of composition, exhibiting a p-type conduction. The thermal conductivity (κ) slightly increased with increasing temperature and showed the lowest value at $R_{Ru/Ca} = 1.0$. The dimensionless figure of merit (ZT) had the maximum at $R_{Ru/Ca} = 1.1$, and the highest ZT value was 0.034 at 1020 K. [doi:10.2320/matertrans.MRA2007055]

(Received March 7, 2007; Accepted April 9, 2007; Published May 25, 2007)

Keywords: *calcium ruthenate, thermoelectric, spark plasma sintering*

1. Introduction

Perovskite-type alkaline-earth metal ruthenium oxides, $SrRuO_3$ (SRO) and $CaRuO_3$ (CRO), have been known as excellent electrical conductors. These materials have been applied as buffer layers in a superconductor-normal metals-superconductor (SNS) Josephson junction[1] and as electrical conducting pastes.[2] $ARuO_3$ (A = Ca and Sr) compounds show metallic electrical conductivity,[1–3] associating with d-electrons from the three-dimensional network corner-sharing RuO_6 octahedra. SRO can be ferromagnetic below 165 K whereas CRO has not been confirmed to be either para- or ferro-magnetic material.[3] The electrical conductivity of CRO[4,5] and SRO[4–6] single crystals were around 4×10^5 Sm^{-1} and 5×10^5 Sm^{-1}at room temperature, respectively. The magnetic and electrical properties of SRO and CRO may be related to their crystal structures, which are orthorhombically distorted $GdFeO_3$ type with *P*nma and *P*bnm space group, respectively.[7] CRO has much more distorted structure than SRO,[7,8] and therefore some characteristic properties of CRO may be expected.

Since $ARuO_3$ is a good electrical conductor with specific crystallographic characteristics, they might be potential thermoelectric materials. Recently, Tsuchida et al.[9] reported that the thermoelectric power factor of CRO increased with increasing temperature showing the highest value among perovskite-structure oxides (330×10^{-6} Wm^{-1} K^{-2} at 1023 K). Several researchers have investigated the electrical property of CRO thin films prepared by sol-gel,[10] sputtering[11] and pulsed laser ablation.[12] Scotti di Uccio et al.[11] proposed that CRO films prepared by sputtering would contain excess Ca resulting in the increase in unit cell volume. The excess Ca might have also resulted in the decrease in electrical conductivity. However, the measurement of electrical properties and crystallographic analysis of dense bulk materials would be more reliable than those of thin films. Therefore, dense CRO bulk body should be investigated to understand the intrinsic nature of CRO.

The thermoelectric property of CRO body has not been studied in detail because dense CRO sintered body cannot be obtained by conventional sintering mainly due to the evaporation of RuO_3.[13] It is known that spark plasma sintering (SPS) can be available to obtain dense bodies by using non-sinterable powder in conventional sintering process. In the present study, dense CRO body was prepared by spark plasma sintering (SPS), and the effect of Ru/Ca ratio on the crystal structure, electrical properties and thermoelectric properties was investigated.

2. Experimental

$CaRuO_3$ powder was synthesized by solid state reaction using $CaCO_3$ (99.99%) and RuO_2 (99.99%) in the molar ratio of Ru to Ca ($R_{Ru/Ca}$) between 0.5 and 1.4. The powder mixtures were calcined at 1273 K for 43.2 ks in air. The calcined powder was compacted in a graphite die and sintered by SPS at 1523 K for 0.3 ks in a vacuum at 80 MPa. The sintered body was cut to $2 \times 2 \times 10$ mm for measuring electrical conductivity by a d.c. 4-probe method and Seebeck coefficient by a thermoelectric power (ΔE)-temperature difference (ΔT) method. Specimens of 10 mm in diameter and 1 mm in thickness were employed to measure thermal conductivity by a laser flash method (ULVAC TC-7000). All electrical and thermal measurements were conducted from room temperature (RT) to 1023 K. The phase and crystal structure were examined by X-ray diffraction (Rigaku Geigerflex). The density (d) was determined by an Archimedes method.

3. Results and Discussion

Figure 1 shows the XRD patterns of Ca-Ru-O compounds at $R_{Ru/Ca} = 0.5$ to 1.4. At $R_{Ru/Ca} = 1.0$, CRO in a single phase was obtained. Second phases of CaO and RuO_2 were identified at $R_{Ru/Ca} = 0.8$ and 1.2, respectively. The volume fraction of second phases, CaO and RuO_2, increased with detaching from $R_{Ru/Ca} = 1.0$. Although Ca_2RuO_4 and $Ca_3Ru_2O_7$ are represented in a phase diagram, these phases

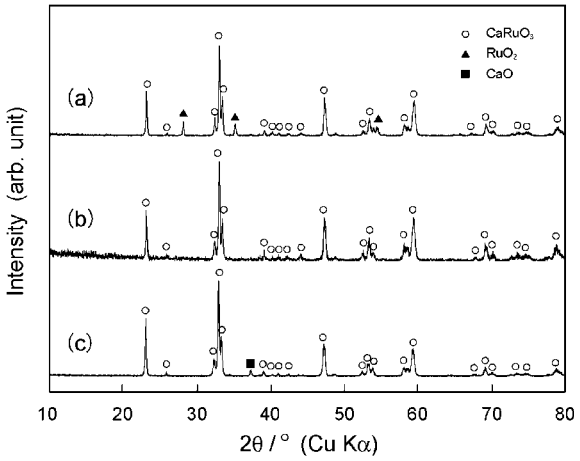

Fig. 1 XRD pattern of sintered Ca-Ru-O compounds with different $R_{Ru/Ca} = 0.8$ (a), 1.0 (b) and 1.2 (c).

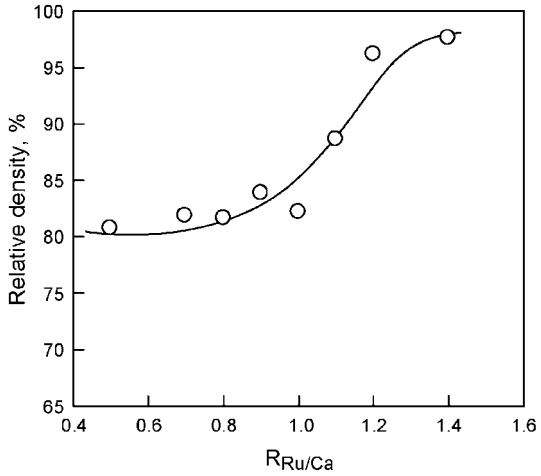

Fig. 2 Effect of $R_{Ru/Ca}$ on the relative density of Ca-Ru-O compounds.

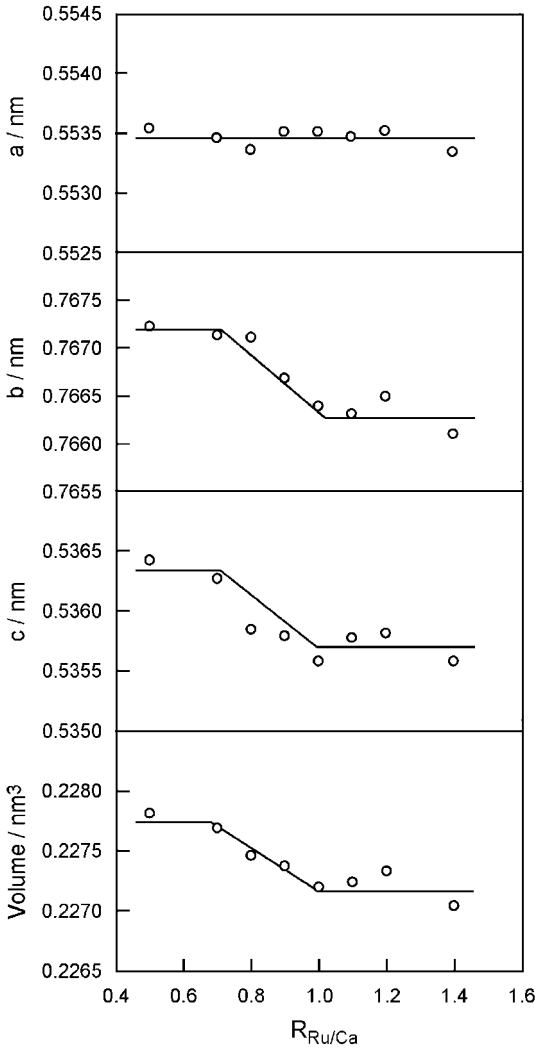

Fig. 3 Effect of $R_{Ru/Ca}$ on lattice parameters and unit cell volume of Ca-Ru-O compounds.

were not identified in the present study. These phases would have formed at a higher sintering temperature.[14)]

Figure 2 shows the relationship between the relative density and $R_{Ru/Ca}$. The density at $R_{Ru/Ca} = 0.5$ to 1.0 ranged between 80 and 85%, and slightly increased with increasing $R_{Ru/Ca}$. At $R_{Ru/Ca} > 1.0$ the density significantly increased with increasing $R_{Ru/Ca}$. The second phase of RuO_2 might cause the increase in density.

Figure 3 demonstrates the effect of $R_{Ru/Ca}$ on the lattice parameters and unit cell volume. The length of a axis was independent of $R_{Ru/Ca}$, and was almost constant value of 0.5535 nm. The lengths of b and c axes decreased from 0.7672 to 0.7663 nm and from 0.5364 to 0.5356 nm with increasing $R_{Ru/Ca}$ from 0.7 to 1.0, respectively. The lattice parameters were constant with further increasing $R_{Ru/Ca}$. The unit cell volume also changed with $R_{Ru/Ca}$, suggesting a solid solution range between $R_{Ru/Ca} = 0.7$ and 1.0. The unit cell volume at $R_{Ru/Ca} = 0.5$ was 0.26% greater than that at the stoichiometric composition. The trend of increase in the unit cell volume with increasing Ca content was similar to that of thin film reported by Scotti di Uccio.[11)] However, the unit cell volume change of thin film was around 8% at $R_{Ru/Ca} = 0.5$. The lattice parameters of bulk materials can be intrinsic behavior whereas thin films may be significantly stressed mainly from the thermal expansion mismatch between film and substrate. The chemical composition of bulk materials would be more precise than that of thin films because of large volume. Therefore, the trend of lattice parameter change as the function of $R_{Ru/Ca}$ would be more reliable than that of thin films.

Figure 4 shows the temperature dependence of electrical conductivity (σ) of Ca-Ru-O compounds at various $R_{Ru/Ca}$. The electrical conductivity decreased with increasing temperature, implying metallic conduction. The σ slightly decreased with increasing temperature at $R_{Ru/Ca} < 1.0$, whereas the decrease in σ was significant at $R_{Ru/Ca} > 1.1$. The σ of stoichiometric CRO was 1.8×10^5 Sm^{-1} at 293 K. The σ of stoichiometric SRO was higher than that of stoichiometric CRO but lower than CRO at $R_{Ru/Ca} > 1.1$. The σ increased with increasing $R_{Ru/Ca}$. At $R_{Ru/Ca} > 1.1$, the σ was much higher than that at $R_{Ru/Ca} < 1.0$. This might be caused by the second phase of RuO_2 because of its high conductivity (1.4×10^6 Sm^{-1} at 293 K). Raming et al.[15)] reported that YSZ (Y_2O_3-stabilized ZrO_2)-RuO_2 composite had high electrical conductivity due to agglomerated RuO_2. However, the second phase of CaO in CRO at $R_{Ru/Ca} < 1.0$

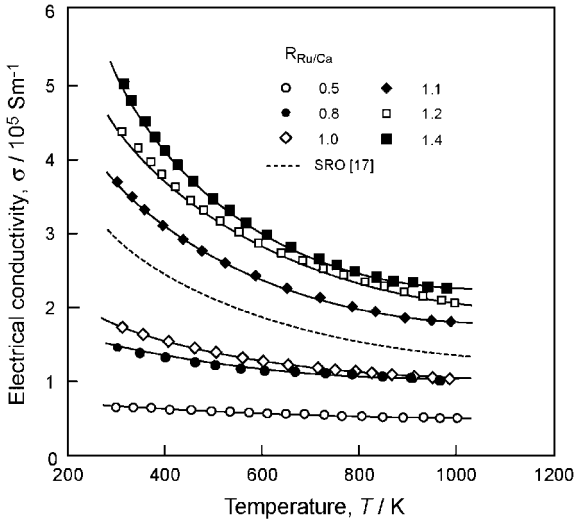

Fig. 4 Temperature dependence of electrical conductivity of Ca-Ru-O compounds.

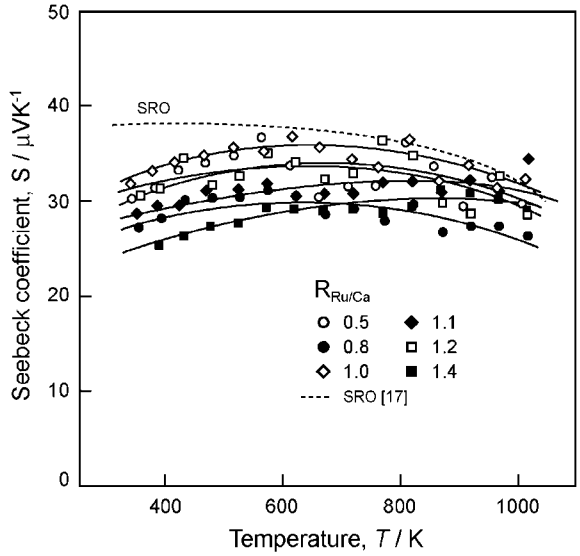

Fig. 6 Temperature dependence of Seebeck coefficient of Ca-Ru-O compounds.

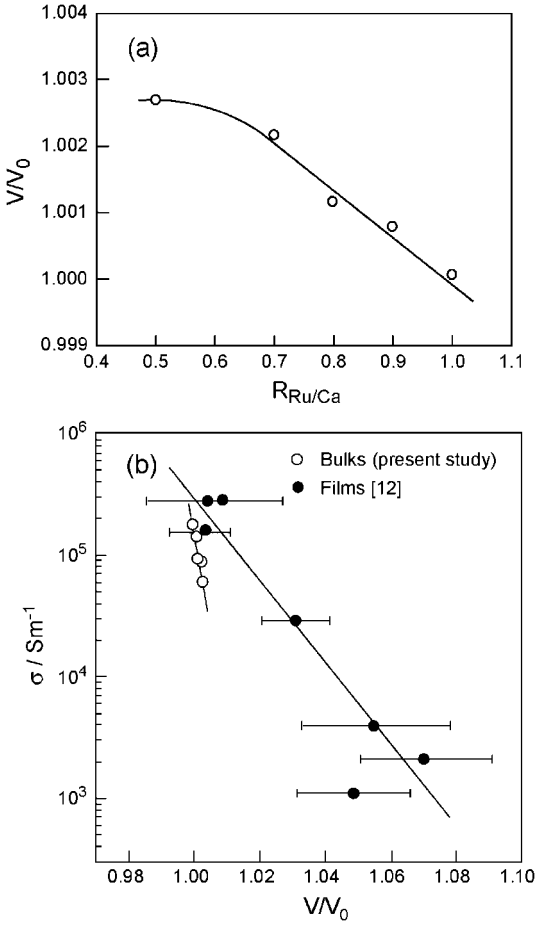

Fig. 5 (a) Effect of $R_{Ru/Ca}$ on unit cell volume change and (b) relationship between unit cell volume change and log σ at room temperature of Ca-Ru-O compounds. (V_o denotes the volume of $CaRuO_3$ at $R_{Ru/Ca} = 1.0$).

may result in the decrease in σ because CaO is an insulating material ($<10^{-8}\,Sm^{-1}$ at 293 K).[16] The change of unit cell volume of CRO at $R_{Ru/Ca} = 0.5$ to 0.9 might be also associated with the decrease in σ.

Figure 5 exhibits the relationship between the unit cell volume (V) and electrical conductivity at room temperature in the Ca-rich region ($R_{Ru/Ca} = 0.5$ to 0.9). The ratio of the unit cell volume in the Ca-rich region (V) to that at $R_{Ru/Ca} = 1.0$ (V_0) increased with decreasing $R_{Ru/Ca}$ from 1.0 to 0.7 (Fig. 5(a)). The log σ linearly decreased with increasing V/V_0 (Fig. 5(b)). This trend was consistent with that reported in the CRO thin film by Scotti di Uccio et al.[11] However, the change of σ in the present bulk CRO body was more significant than that of CRO thin film. Since the electrical conduction of CRO may be closely related with the connection of RuO_6 octahedra, the increase in unit cell volume could cause the less electrical conductivity.

Figure 6 represents temperature dependence of Seebeck coefficient (S) of CRO at various $R_{Ru/Ca}$. The value of SRO was included as comparison. All specimens showed positive Seebeck coefficient, implying a p-type conduction. The S of CRO was 25 to 35 μVK^{-1}, almost independent of $R_{Ru/Ca}$ and temperature from RT to 1020 K. The CRO at $R_{Ru/Ca} = 1.0$ had the highest S in the whole temperature range. The S of SRO was around 30 to 40 μVK^{-1},[17] which was slightly higher than that of CRO.

Figure 7 shows the temperature dependence of power factor ($P = S^2\sigma$) of CRO and SRO. The P of CRO at the stoichiometric composition decreased from 165 to $110 \times 10^{-6}\,Wm^{-1}\,K^{-2}$ with increasing temperature from RT to 1020 K. This value was lower than that of SRO. The P of CRO at $R_{Ru/Ca} = 1.1$ was almost the same as that of SRO. The P of CRO and SRO both similarly decreased with increasing temperature. On the other hand, the P of CRO reported by Tsuchida et al.[9] increased with increasing temperature. This trend might not be the intrinsic nature of CRO because the σ of $ARuO_3$ would generally decrease with increasing temperature and the S would be independence of temperature. Since CRO cannot be fully densified by conventional sintering, some grain boundary effects might have affected to the unusual trend.

Figure 8 shows temperature dependence of thermal conductivity (κ) of CRO with various $R_{Ru/Ca}$ and SRO.[17] The κ

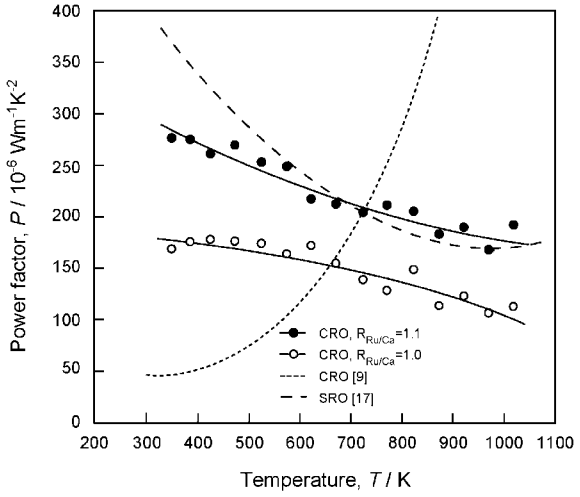

Fig. 7 Temperature dependence of power factor of Ca-Ru-O compounds.

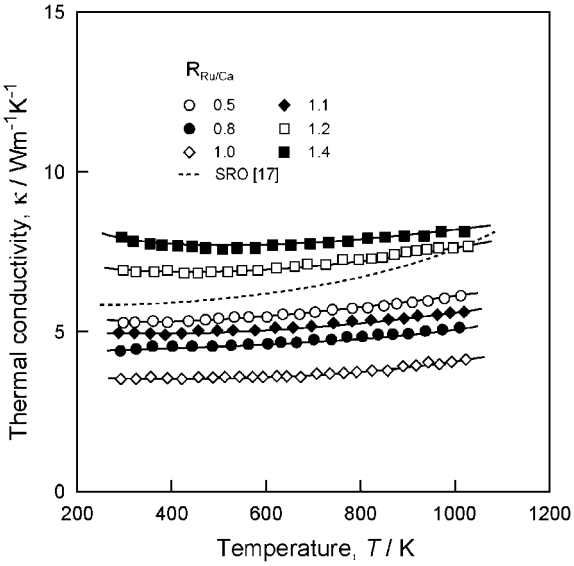

Fig. 8 Temperature dependence of thermal conductivity of Ca-Ru-O compounds.

of CRO increased slightly with increasing temperature. The lowest κ ranged around 3.5 to 4.0 $Wm^{-1} K^{-1}$ at the $R_{Ru/Ca} = 1.0$ from 293 to 1020 K. The κ decreased from 5.3 to 3.5 $Wm^{-1} K^{-1}$ with increasing $R_{Ru/Ca}$ from 0.5 to 1.0, and increased from 6.6 to 8.0 $Wm^{-1} K^{-1}$ with further increasing $R_{Ru/Ca}$ at RT. This might be resulted from the effect of second phase of RuO_2 and CaO because their thermal conductivities would be several times greater than that of CRO as shown in Table 1. The κ of SRO slightly increased with increasing temperature around 6 to 8 $Wm^{-1} K^{-1}$ from RT to 1200 K. These values were less than that of CRO at $R_{Ru/Ca} > 1.2$ whereas higher than that of $R_{Ru/Ca} < 1.1$.

Table 1 summarizes the lattice parameters and thermoelectric properties of CRO and SRO prepared by different methods. A tolerance factor (t) is defined to evaluate the geometric distortion of crystal structure. The t of crystal structure without distortion is 1. The t of $CaRuO_3$ is 0.88 and that of $SrRuO_3$ is 0.95. Kobayashi et al.[8] reported that the electrical conductivity decreased with decreasing the t. The lattice parameters of CRO prepared by SPS were slightly higher than that of single crystal. Furthermore, with decreasing $R_{Ru/Ca}$ from 1.0 to 0.7 the lattice parameters of CRO increased and the σ decreased. The increase in lattice parameter might result in the increase in the distortion degree *(t)*. The crystal structures of $Bi_{2-x}Ln_xRu_2O_7$ and $Pb_{2-x}Ln_xRu_2O_{7-d}$ (Ln = Y, Pr-Lu) pyrochlores are known to be similar to the $GdFeO_3$-type perovskite structure having a framework of corner-sharing RuO_6 octahedra. Kanno et al.[18] reported that the σ of the pyrochlores decreased with increasing x, suggesting the increase in the distortion of the RuO_2 octahedra and the increase in the length of the Ru-O bonds and RuO_6 zigzag chains. Therefore, the decrease in the σ of CRO at $R_{Ru/Ca} < 1.0$ may be associated with the distortion of crystal structure and the increase in the Ru-O bond length and the RuO_6 zigzag chains. So far, no reports on the Seebeck coefficient and thermal conductivity of CRO have been published. The S and σ of CRO were slightly smaller than these of SRO. However, the κ was almost a half of SRO, resulting in the higher thermoelectric figure of merit than that of SRO.

Figure 9 shows the temperature dependence of dimensionless thermoelectric figure of merit (ZT) calculated from eq. (1).

$$ZT = S^2\sigma T/\kappa \quad (1)$$

The ZT values of CRO at $R_{Ru/Ca} = 1.0$ and 1.1 slightly increased with increasing temperature, and were greater than

Table 1 Characteristics and physical properties of $CaRuO_3$ and $SrRuO_3$.

Structure/ space group	Lattice parameters (nm) a	b	c	Tolerance factors	σ (Sm^{-1}) at RT	Seebeck coefficient (μVK^{-1})	Thermal conductivity ($Wm^{-1} K^{-1}$)	Method/Ref
$CaRuO_3$	0.5535	0.7663	0.5355*	0.88[8]	1.8×10^5*	25–35*	3.5–4.0*	SPS*
Orthorhombic/					0.2×10^5[19]	—	—	Pressureless[19]
*P*nma[7]	0.5528	0.7660	0.5355[4]		4.0×10^5[4,5]	—	—	Single crystal[4,5]
$SrRuO_3$	0.557	0.555	0.787[17]	0.95[8]	2.6×10^5[18]	30–40[21]	6.0–8.0[21]	SPS[21]
Orthorhombic/					0.7×10^5[20]	—	—	Pressureless[20]
*P*bnm[7]	0.5572	0.5531	0.7849[4]		5.0×10^5[4,6]	—	—	Single crystal[4–6]
RuO_2					14.0×10^5*	—	13.0–23.0*	SPS*
CaO					$<10^{-8}$	—	14.84 (RT)	[16]

*: present study

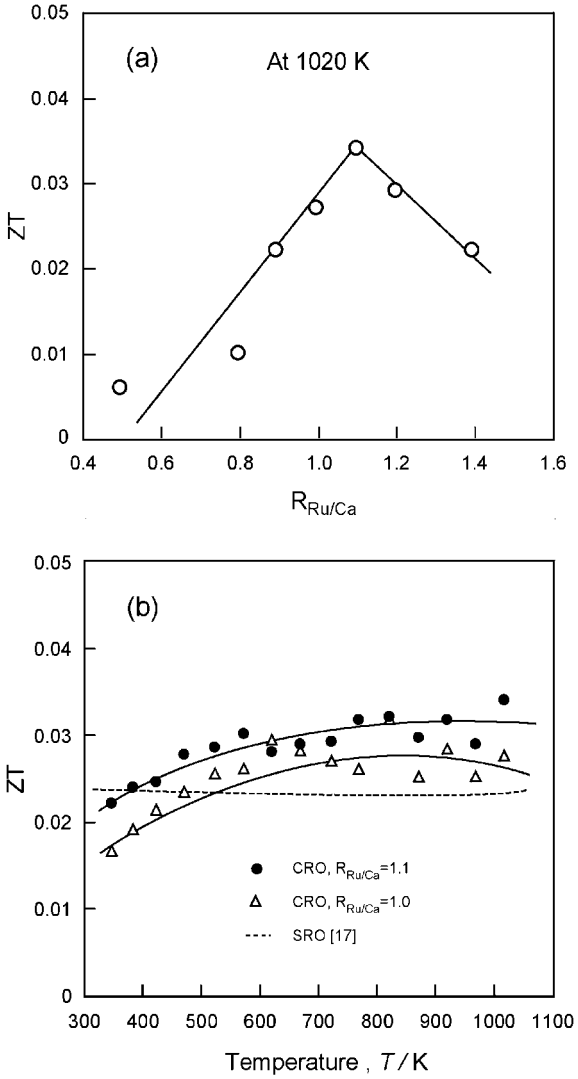

Fig. 9 Effect of $R_{Ru/Ca}$ at 1020 K (a) and temperature (b) on ZT of Ca-Ru-O compounds.

that of SRO[17] from 600 to 1020 K. The CRO had higher *ZT* than SRO because of the lower thermal conductivity. The *ZT* value at 1020 K increased with increasing $R_{Ru/Ca}$ up to 1.1 and showed maximum value of 0.034, and then decreased to 0.023 with increasing $R_{Ru/Ca}$ to 1.4 (Fig. 9(a)). The CRO at $R_{Ru/Ca} = 1.1$ had the highest *ZT* in the whole temperature range (Fig. 9(b)).

4. Conclusion

Ca-Ru-O compounds in various molar ratios of Ca to Ru ($R_{Ru/Ca}$) from 0.5 to 1.4 were prepared by SPS. $CaRuO_3$ (CRO) in a single phase was obtained at $R_{Ru/Ca} = 1.0$, whereas second phases of CaO and RuO_2 were identified at $R_{Ru/Ca} < 0.8$ and $R_{Ru/Ca} > 1.1$, respectively. The relative density was higher than 80% and increased with increasing $R_{Ru/Ca}$. The lattice parameters of CRO changed continuously at $R_{Ru/Ca} = 0.7$ to 1.0, implying a non-stoichiometric range of CRO. The electrical conductivity exhibited metallic conduction and increased with increasing $R_{Ru/Ca}$. The Seebeck coefficient was almost independent of temperature and $R_{Ru/Ca}$ with the values of around 25 to 35 μVK^{-1} indicating a p-type conduction. The thermal conductivity (κ) slightly increased with increasing temperature. At $R_{Ru/Ca} = 1.0$, the κ was the lowest around 3.5 to 4.0 $Wm^{-1}K^{-1}$. The highest dimensionless figure of merit (*ZT*) was 0.034 at 1020 K at $R_{Ru/Ca} = 1.1$.

Acknowledgement

The authors are grateful to JSPS-KOSFF Asian CORE program and Furuya Metal Co., Ltd. for financial support.

REFERENCES

1) K. Char, M. S. Colclough, T. H. Geballe and K. E. Myers: Appl. Phys. Lett. **62** (1993) 196–198.
2) K. Gurunathan, N. Vyawahare and D. P. Amalnerkar: J. Mater. Sci.: Materials in Electronics **16** (2005) 47–56.
3) I. Felner, I. Nowik, I. Bradaric and M. Gospodinov: Phys. Rev. B **62** (2000) 11332–11335.
4) R. J. Bouchard, J. L. Gillson and E. I. du Pont de Nemours: Mater. Res. Bull. **7** (1972) 873–878.
5) L. Capogna, A. P. Mackenzie, R. S. Perry, S. A. Grigera, L. M. Galvin, P. Raychaudhuri and A. J. Schofield: Phys. Rev. Lett. **88** (2002) 076602-1–076602-4.
6) P. B. Allen, H. Berger, O. Chauvet, L. Forro, T. Jarlborg, A. Junod, B. Revaz and G. Santi: Phys. Rev. B **53** (1996) 4393–4398.
7) M. V. Rama Rao, V. G. Sathe, D. Sornadurai, B. Panigrahi and T. Shripathi: J. Phys. Chem. Solids **62** (2001) 797–806.
8) H. Kobayashi, M. Nagata, R. Kanno and Y. Kawamoto: Mater. Res. Bull. **29** (1994) 1271–1280.
9) K. Tsuchida, Y. Tanaka, T. Ifuku, Y. Nakao, T. Matsuda, S. Nagashima, H. Maeda and A. Kato: Korean J. Chem. Eng. **13** (1996) 478–481.
10) S. Yamada, N. Fukuoka, T. Taniguchi, T. C. Ozawa, Y. Nagata, T. Uchida and H. Samata: Thin Solid Films **478** (2005) 1–5.
11) U. Scotti di Uccio, F. Bevilacqua, G. G. Condorelli, G. Mascolo, F. Ricci and F. Miletto Granozio: Europ. J. Phys. B **41** (2004) 3–9.
12) S. G. Lee, K. Park, Y. K. Park and J.-C. Park: Appl. Phys. Lett. **64** (1994) 2028–2030.
13) W. E. Bell and M. Tagami: J. Phys. Chem. **67** (1963) 2432–2436.
14) K. T. Jacob, K. T. Lwin and Y. Waseda: J. Electrochem. Soc. **150** (2003) E227–E232.
15) T. P. Raming, W. E. van Zyl and H. Verweij: Chem. Mater. **13** (2001) 284–289.
16) H. H. Glascock, Jr. and E. B. Hensley: Phys. Rev. **131** (1963) 649–652.
17) T. Maekawa, K. Kurosaki, H. Muta, M. Uno and S. yamanaka: J. Alloy and Compd. **387** (2005) 56–59.
18) R. Kanno, Y. Takeda, T. Yamamoto, Y. Kawamoto and O. Yamamoto: J. Solid State Chem. **102** (1993) 106–114.
19) F. P. de la Cruz, N. E. Massa, V. M. Nassif, S. L. Cuffini, R. E. Carbonio and H. Salva: Phys. Stat. Sol. (b) **220** (2000) 603–607.
20) J. J. Neumeier, A. L. Cornelius and J. S. Schilling: Physica B **198** (1994) 324–328.